East European Journal of Physics. **2.** 206-214 (2023)
DOI:10.26565/2312-4334-2023-2-22 ISSN 2312-4334

IMPROVEMENT OF THE SHIELDING EFFECTIVENESS OF PMMA/MWCNTS/Ag HYBRID COMPOSITE FOR X-BAND APPLICATION[†]

Badiaa Ismal Alawi, Nadia Abbas Ali*
Department of Physics, College of Science, University of Baghdad, Baghdad, Iraq
**Corresponding author: nadia.ali@sc.uobaghdad.edu.iq*
Received March 10, 2023; revised March 21, 2023; accepted March 27, 2023

Herein, the Polymethyl Methacrylate/Mutiwalled Carbon Nanotube/Silver (PMMA/MWCNT/Ag) hybrid composite films are prepared by solvent casting method to be used in an electrical application. The AC conductivity and dielectric characteristics have been investigated at room temperature. The electrical conductivity of the hybrid composite reaches a percolation critical concentration of 2.14×10^{-4} S/cm by Ag doping. For all PMMA/MWCNT/Ag hybrid composites, the frequency-dependent dielectric constant decreases as the frequency area widens. As the concentrations of MWCNT and Ag increase, the AC conductivity exhibits an increasing trend. The MWCNT and Ag content was found to significantly affect the SE of the given composites. A high electromagnetic (EM) shielding efficiency (SE) was achieved between 8.2 and 12.4 GHz (X-band). The highest EM attenuation of 18 dB at 12 GHz was achieved using 0.5 wt% MWCNT and Ag. The thermal analysis of the formed PMMA/MWCNT/Ag hybrid composites showed that exothermic reactions with the greatest weight loss took place between 200°C and 300°C. Field emission scanning electron microscope (FESEM) show that PMMA/MWCNT/Ag hybrid composites had uniform dispersion of the carbon nano tube and silver particles within the PMMA matrix.
Keywords: *Electromagnetic interference shielding; X-band; Electrical conductivity; Dielectric constant; Dielectric loss; Thermal analysis*
PACS: 72.15.Cz; 77.22.Gm, 73.22.f

INTRODUCTION

An electromagnetic interference (EMI) barrier, preventing the radiation from flowing through it, is formed when electromagnetic radiation is reflected or absorbed by a substance [1]. Nowadays, protecting against EMI is essential in the world of electronic systems and components. In the 8.2 to 12.4 GHz (X-band) range, the EMI shielding is very important for both industrial and military applications, systems for Doppler, weather radar, TV picture transmission, and telephone microwave [2,3]. Thermoplastics like polycarbonate (PC), polypropylene (PP), polyethylene (PE), polystyrene (PS), polylactide (PLA), polymethylmethacrylate (PMMA), acrylonitrile butadiene styrene (ABS), or polyvinylidene fluoride (PVDF) and thermosets like epoxy resins, polydimethylsiloxane (PDMS), or polyurethane (PU) are two types of polymer matrices that are frequently utilized for EMI shielding materials [4]. There are a variety of conductive fillers that can be used for functionalizing cork-polymer composites (CPC) such as metal fillers like steel fibers, copper, and silver nanowires, or metal oxide fillers like magnetite ferrite which can be easily spread in various polymer matrices. Amongst, the carbon-based fillers, graphite and carbon black are most typically utilized because of their small weight and strong conductivity [5].

Recently, more research is being done on polymer composites with metallic additives as possible electromagnetic field shielding materials. The metal-filled polymer composites are beneficial because of their low specific weight, good corrosion resistance, plasticity, and straightforward, inexpensive production techniques [6]. A wide range of alterations to polymer composites (in terms of filler type, structure, and content, as well as matrix polymer selection) enables the control of their electromagnetic characteristics for a given application. Polymer composites with metal fillers remain one of the most crucial materials to take into account for EMI shielding applications. In addition, metals like silver, copper, gold, and aluminum are ideal for reflecting light due to their high conductivity [7].

A new type of pollution known as noise, radio frequency interference, electromagnetic radiation, or EMI, which causes equipment to malfunction, has been produced by the expansion of the use of electronic gadgets [8]. The development of polymer composites has revealed a novel carbon-based polymer composite. The carbon nanotubes (CNTs) have demonstrated potential as reinforcement fillers in polymers to improve an EMI shielding material due to their substantial specific surface area, distinct 3D networking structure, and distinctive electrical structure [9]. Silver nanoparticles (Ag-NPs) have a significant impact on the field of nanotechnology and are significant due to their unique optical, electrical, and magnetic properties depending on their particle size [10]. It was also used in electronics, optics, and other fields due to its high conductivity, antibacterial properties, and chemical stability.

The CNTs and Ag-NPs have recently been able to play a significant role in the creation of nano EMI shielding materials thanks to their distinctive electrical, mechanical, and magnetic properties [11]. Research on next-generation EMI shielding materials is now heavily focused on EMI shielding hybrid composites made by combining CNTs and Ag with organic polymers [12]. MWCNT-PMMA composite films have been reported to have up to 27 dB SE for high CNT loadings of around 40 wt% by Kim et al. [13] who researched the EMI shielding capabilities of MWCNT-PMMA

[†] ***Cite as:*** B.I. Alawi, and N.A. Ali, East Eur. J. Phys. **2**, 206 (2023), https://doi.org/10.26565/2312-4334-2023-2-22

films in the range (50 MHz–13.5 GHz). In situ polymerization and ex-situ manufacturing procedures were used to prepare MWCNT-PMMA composites. Yuen et al. [14] investigated the impact of processing variables on the EMI shielding capabilities of these composites. It was reported that the shielding efficiency of EMI of composites prepared by stacking 10 layers of 0.1-mm MWCNT-PMMA films was higher than a single 1-mm thick piece of bulk 4.76 wt% MWCNT-PMMA composite, confirming the composite stacking process as a better fabrication method. In addition, it was deduced that the SE was higher for in situ fabricated composites. Liu et al. [15] showed that PU/SWCNT composites with a 20 wt% SWCNT loading may produce an EMI SE of up to 17 dB in the 8.2-12.4 GHz range. It was deduced that the EMI shielding levels for SWCNT- or MWCNT-polymer composites reported up to this point typically vary between 20 and 30 dB only in the X-band frequency range. Higher values have been seen in the X-band, although at frequencies other than that. Yuan et al. [16] generated electromagnetic absorbent materials based on the PMMA/CNT nanocomposite. The dielectric loss of PMMA/CNT nanocomposite foams rose, with a CNT loading of 4–8 wt %, from 2.1 to 10.8 (X-band). This demonstrates that a conducting network of nanotubes formed in the PMMA matrix as a result of the nanofiller loading. The electrical conductivity of the nanocomposite foam increased as a result, resulting in a dielectric loss. The layered structure is meant to increase the absorption bandwidth of the PMMA/CNT nanocomposite foams. The layered nanocomposite foam's absorption bandwidth was 3.5 GHz. The top layer of the foam had a low dielectric constant due to lower CNT content than the bottom layers, which had higher concentrations of nanofiller. PMMA and single-walled carbon nanotube (SWCNT) nanocomposites were primed by Das et al. [17]. The percolation threshold was increased from 10^{-15} to 10^{-2} by the SWCNT loading. The PMMA/SWCNT percolation threshold was 3 wt%. An improvement in the EMI shielding of 40 dB was seen at 200 MHz in the X-band (8-12 GHz) for 20 wt% SWCNT.

The objective of this study is to investigate the role of MWCNT and Ag as fillers in intrinsically conducting PMMA polymer in altering the EMI shielding performance of polymer hybrids. For this purpose, various ratios of MWCNT and Ag are incorporated into the PMMA to obtain the optimum doping ratio. The chemical structure, electrical conductivity measurement, frequency-dependent dielectric constant, electromagnetic shielding efficiency as well as thermal analysis of the formed polymer hybrids were investigated and discussed.

1. EXPERIMENTAL DETAILS

1.1. Sample preparation

The MWCNT filler, in this work, had a diameter of 20–40 nm and a length of 10–30 μm. The PMMA/MWCNT/Ag hybrid composite films were synthesized by the solvent casting method. In this method, the MWCNT and Ag were ultrasonically dispersed in chloroform for 2 h to form a stable suspension. Then, the suspension was combined with a solution of 3 g PMMA in chloroform to form a combination of PMMA/MWCNT/Ag including 0.1, 0.2, 0.3, 0.4, and 0.5 wt% MWCNT and utilizing a constant ratio of Ag at 0.5 wt%. The mixture was once more ultrasonically processed for 2 h to achieve a consistent dispersion of MWCNTs and Ag in PMMA. Finally, the thin polymer film was cast from this solution by pouring it into a Petri dish covered with Teflon spray (diameter ~ 4 cm). After the solvent had evaporated, the nanocomposite films were allowed to dry at room temperature for a day before being removed from the glass dishes and cut into pieces for characterization and structural analysis. The thicknesses of the formed PMMA/MWCNT/Ag nanocomposite film were measured to be around 0.25 mm.

1.2. Sample characterizations

The chemical bonds in the formed samples were analyzed using the Infrared Fourier Transform (FTIR) Analysis. For this purpose, the FTIR spectroscopy model Shimadzu type FTIR-7600 was used to record the infrared spectra in the wavenumber range from 400 to 4000 cm^{-1}. The electrical characteristics were carried out by evaluating the resistivity (ρ) of the films. The electrical resistance has been measured as a function of temperature (T) in the temperature range of 303-393 K using the following equation [18]: $\rho = RAL$, where R is the electric resistance of the sample, A is the film's cross-sectional area and L is the sample's thickness. From the relationship, the conductivity (σ_{dc}) of the films was calculated: $\sigma_{dc} = \frac{1}{RAL}$. The electrical conductivity, which is determined by the Arrhenius equation and varies exponentially with temperature and is derived by: $\sigma_{dc} = \sigma_0 e^{\frac{-E_a}{k_B T}}$. The total conductivity was calculated from the following equation: $\sigma_t(\omega) = \frac{L}{RA}$. The AC conductivity $\sigma_{ac}(\omega)$ was calculated by using the relation: $\sigma_{tot}(\omega) = \sigma_{ac}(\omega)+\sigma_{dc}$ and $\sigma_{ac}(\omega) = \sigma_t-\sigma_{dc} = A\omega^s$, where σ_{dc} is the DC conductivity, A is a constant independent of temperature, ($\omega = 2\pi f$), and s is the frequency exponent.

The dielectric permittivity of a material (ε) is considered a complex quantity with a real part (ε_r) and imaginary part (ε_i) and is given by [17]: $\boldsymbol{\varepsilon = \varepsilon_r + \varepsilon_i}$. The values of the parallel mode capacitance (C_p) and the loss tangent (tan (δ)) are used to determine the real and imaginary components of the dielectric permittivity or ε_r and ε_i, respectively. For the frequency range of 10 kHz–100 MHz and room temperature, the values of Cp and tan are calculated. The values of r and I are determined using the following equations: $\varepsilon' = C_p d\varepsilon_o A$; $\varepsilon'' = \varepsilon' tan(\delta)$ and $\tan(\delta) = \varepsilon''/\varepsilon'$ where $\delta = 90–\varphi$, d and A are the thickness and cross-sectional area of the sample, respectively, and ε_o is the permittivity of free space.

The electromagnetic properties of the samples are evaluated by the waveguide technique at X-band frequency (closed system). The about 1.3 cm thick preparation samples are cut to fit in the cross-section of the rectangular

waveguide (2.29×1.02 cm^2). The sample is positioned inside the waveguide (sample holder) so that it completely encloses the cross-section to prevent any EM radiation leakage. The incident and transmission energy between 8.2-12.4 GHz is utilized to determine the shielding effectiveness. The SE of the PMMA/MWCNT/Ag hybrid composite was measured using a network analyzer and the coaxial line technique following ASTM D4935-99 [19] in the frequency range of 8.2 to 12.4 GHz (X-band). The sum of the contributions from absorption loss (SE_A), reflection loss (SE_R), and multiple reflections (SE_M) may be used to describe SE (SE_{total}) [20]. The value of SE was determined and represented in decibels (dB) using the following equation: $SE_{total} = SE_A + SE_R + SE_M$.

There are descriptions of measuring the glass and various polymer transitions. A hypothesis explaining how a glass transition appears in a Differential Thermal Analysis device (DTA) thermogram and how to extract the thermogram's true value is provided. The thermal analysis and thermal stability of the investigated samples were carried out using the DTA model a TG-209F with a heating rate of 10 °C/min under nitrogen flowing at a rate of 50 ml/min. For this purpose, around 10–19 mg of the samples were provided at thermal degradation temperatures of 25–400°C. Field emission scanning electron microscopy (FESEM) provides topographical and elemental information at magnifications of 10× to 300,000×.

2. RESULTS AND DISSECTION

The FTIR spectra provide information on the functional groups and chemical structure of the investigated materials. The FTIR spectrum of pure PMMA film as well as PMMA/MWCNT/Ag nanocomposites are shown in **Fig. 1**.

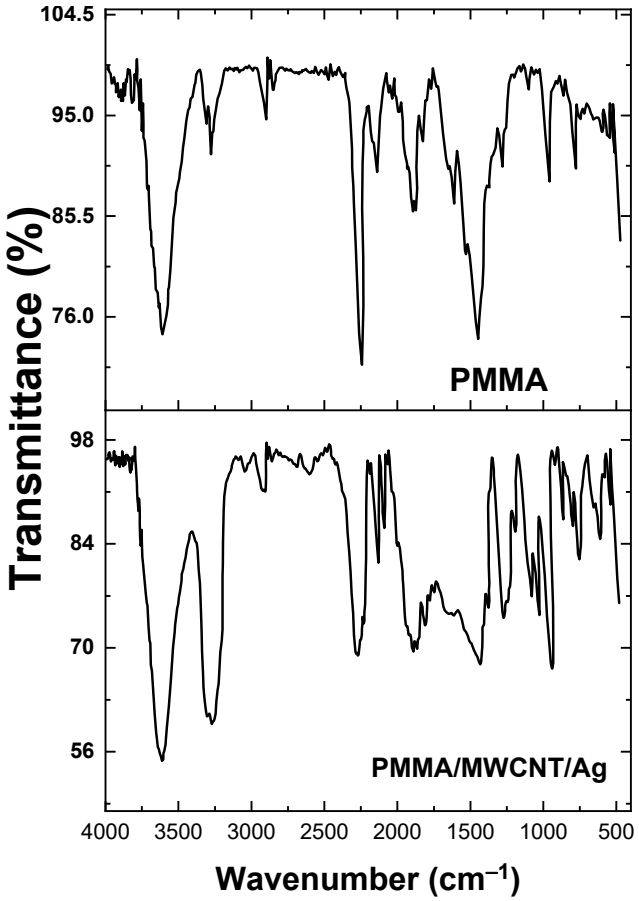

Figure 1. FTIR spectra for pure PMMA and PMMA/MWCNT/Ag hybrid composites.

For pure PMMA, the left region, between 1500 and 4000 cm^{-1}, is referred to as the diagnostic region, and the second, between 400 and 1500 cm^{-1}, is referred to as the fingerprint region that points to the functional group region. The left region is particularly close to 4000 cm^{-1} because it is for the high energy bonds. The O-H stretching vibration is represented by the peak at 3414 cm^{-1}, while the C=O stretching vibration from PMMA is characterized by the absorption band at 1732 cm^{-1}. The C-O stretching vibration in PMMA is shown by the absorption band at 1147 cm^{-1}. The absorption band at 1242 cm^{-1} indicates C-C from PMMA, while the absorption band at 2951 cm^{-1} corresponds to C-H stretching in that area. A strong peak at 1736 cm^{-1} was seen belonging to the ester carbonyl group's (C=O) stretching vibration. The large peak between 1260 and 1000 cm^{-1} can be attributed to the stretching vibration of the C-O (ester bond). The bending of C-H is what causes the broadband from 950-481 cm^{-1}. It is possible to attribute the peak at 2935 cm^{-1} to -CH stretching, which is consistent with other work [17].

The FTIR spectrum for PMMA/MWCNT/Ag hybrid composite exhibits three distinct peaks, C=O, O-H, and C-O. These peaks are the result of oxidation forming the COOH groups on the surface of MWCNTs, which demonstrated an aromatic skeletal vibration (C=C stretching) at 1615 cm^{-1}. The absorption band observed at 1540 cm^{-1} is more likely from the C=C stretching mode of CNTs. The C=O stretch of the -COOH group is responsible for the peak that was seen at 1731 cm^{-1}. Stretching vibrations are responsible for the wide peak between 4000 and 2900 cm^{-1}, while the peak at 1195 cm^{-1} is due to -O-CH_3 stretching vibrations. Peaks for C=C stretching and O-H broadening stretching are located at 1660 and 3307 cm^{-1}, respectively. Due to the existence of ester carbonyl group stretching vibration, or C=O stretching, a peak was visible at 1872 cm^{-1}. The stretching vibration of the C-O (ester bond) can be used to explain the wide peak spanning from 1260 to 1000 cm^{-1}. The peak for N-H stretching is at 3394 cm^{-1}, followed by C-O stretching at 1731 cm^{-1}, C-H bending at 1057 cm^{-1}, and C-O stretching at 3433 cm^{-1}. The absorption bands for O-H bending and C-O stretching are at 1410 cm^{-1} and 1090 cm^{-1}, respectively. The peaks at 2920 and 2850 cm^{-1} are connected to the C-H stretching mode, whereas the strong peak at 3440 cm^{-1} is related to the O-H stretching of the hydroxyl group. The principal silver peaks were seen at 2927, 1631, and 1383 cm^{-1}. A distinct and powerful absorption band at 1631 cm^{-1} was visible in the spectra and was identified as the

stretching vibration of the (NH) C=O group. A band at 1383 cm^{-1} was created for the stretching of C-C and C-N; while a strong peak at 2927 cm^{-1} was attributed to the stretching vibrations of C-H and C-H (methoxy compounds).

The DC electrical conductivity (σ) for PMMA/MWCNT/Ag hybrid composite films for various ratios of MWCNT and Ag at a temperature range of 30-120 °C is shown in **Fig. 2**. The findings indicate that the value of for PMMA was around 1.1×10^{-9} ($S\cdot cm^{-1}$) and the value of for PMMA/MWCNT/Ag is shown in **Table 1**.

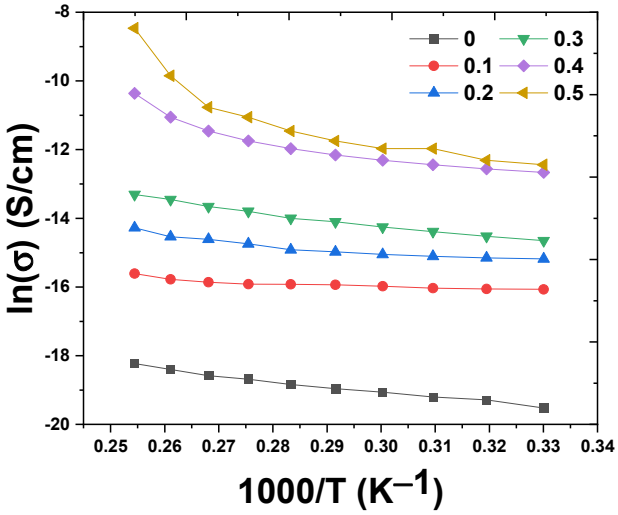

Figure 2. Electrical conductivity (σ) versus ($\frac{10^3}{T}$) for pure PMMA and PMMA/MWCNT/Ag hybrid composites with ratios of MWCNTs of 0.1, 0.2, 0.3, 0.4, and 0.5 wt%.

Table 1. Electrical conductivity (σ) and activation energy (E_a) for electrical transition, the exponential factor (s) for PMMA/MWCNT/Ag hybrid composites.

MWCNT ratio (wt%)	**0**	**0.1**	**0.2**	**0.3**	**0.4**	**0.5**
σ (S/cm)	3.21×10^{-9}	1.05×10^{-7}	2.54×10^{-7}	1.01×10^{-6}	1.57×10^{-5}	2.15×10^{-4}
E_a (eV)	2.36	2.1	2.09	1.96	1.88	1.52
S	0.94	0.66	0.64	0.63	0.55	0.39

The following may be used to explain why PMMA/MWCNT/Ag hybrid composite films have increased d.c electrical conductivity: The presence of MWCNTs and Ag as filler in the PMMA matrix aids in the creation of broad conductive networks that enable the movement of electrons inside the composite and that MWCNTs induce the current to flow even if there are no direct connections between MWCNTs. The electrons can travel through the insulator with a certain probability between conductive components (MWCNTs) in a process known as "quantum mechanical tunneling". In addition, electrons can go between conductors by "tunneling" through the insulating layer to put it another way. A low percolation threshold and conventional percolating network characteristics were displayed by the carbon nanotube network. Although silver has high conductivity qualities, metal is costly and bulky [6]. With a high aspect ratio and distinctive conductivity, MWCNTs have mostly been utilized as conductive fillers up until this point due to their low density.

The insulating PMMA matrix becomes conductive plastic when MWCNT is added, as seen in **Fig. 2**. The loading of MWCNT from 0.1 to 0.5 wt%, and 0.5 wt% Ag increased the electrical conductivity of the PMMA. Only 0.5% of MWCNT/Ag added to PMMA produced conductivities as high as 2.15×10^{-4} S/cm. The conductivity was enhanced in a traditional percolating manner with a percolation threshold of roughly 0.5 wt% due to the widespread usage of used Ag as a conductor wire in circuits that call for high conductivity. Although individual MWCNTs have great characteristics, their microscale length necessitates electron percolation from one CNT to another, often thousands of times. The greater resistance of the MWCNT-MWCNT junction significantly lowers the electron mean free path, lowering the electrode's conductivity. The Ag-NPs are the most well-known choices for enhancing MWCNT network conductivities due to their high conductivity, chemical stability, and compatibility with sintering even at low temperatures.

The table illustrates the link between $\ln(\sigma_{dc})$ and the inverse absolute temperature of nanocomposites. From the fitted lines the slope can be used to characterize the activation energy (E_a), and the findings revealed that the PMMA-/MWCNT/Ag hybrid composite reduced the activation energy values of samples owing to the effect of the space charge, with high values E_a ranging from 2.36 eV to 1.52 eV. In the prohibited energy gap, it also generates local energy levels that interact to trap charge carriers that jump between levels, and the conduction process lowers the concentration of hopping. The activation energy is low for PMMA/MWCNT/Ag at (0.5 wt%) due to the formation of a continuous network of carbon nanotubes and silver inside the hybrid composite that contains routes that aid charge carriers in passing through, and it decreases as the loading ratio of MWCNT and Ag increases. The voids in the carbon nanotube network must be bridged with another conductive material, such as silver, which has no voids, or at least with

a much smaller scale void pattern that has high transparency, high conductivity, and solution processability [15]. This will also result in low sheet resistance and a uniform conductive film.

AC Conductivity

Figure 3 shows the AC electrical conductivity of PMMA for 10 kHz to 10 MHz at room temperature along with different amounts of MWCNT and Ag integrated. The MWCNT and Ag network's connection and electron transport mechanism in the polymeric matrix is revealed by the hybrid composites' AC conductivity. It has been shown that all samples' conductivities rise with frequency, however, PMMA's conductivity is lower than that of its MWCNT, Ag. This may be explained by dipoles' propensity to point in the direction of the applied field in polymeric materials [11,12].

The AC conductivity is derived by subtracting the AC conductivity from the total conductivity. **Figure 3** depicts the frequency dependence of AC conductivity. The graph clearly shows that as frequency increases, a.c. increases. One may determine the frequency exponent (s), which is less than one, by computing the slope of the straight lines in **Fig. 3**. The average values of (s) appear to be consistent with protons acting as charge carriers that hop across polymer chains.

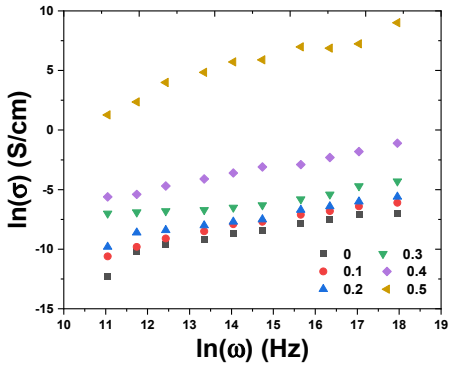

Figure 3. ln(σ) versus ln (ω) for pure PMMA and PMMA/MWCNT/Ag hybrid composites with ratios of MWCNTs of 0.1, 0.2, 0.3, 0.4, and 0.5 wt%.

The hybrid composite including MWCNT/Ag (0.1-0.4/0.5 wt%) demonstrates frequency-dependent conductance and is within the percolation threshold, except for its conductance being an order of magnitude larger. At low filler loading, there is not enough filler to form a conductive network; hence, AC conduction occurred via the tunneling current. The percolation threshold was likely created by the interaction of the nanotubes and silver to create conductive pathways, and the increase in AC conductance is attributed to the leakage current, according to a significant rise in conductance at MWCNT/Ag (0.5/0.5 wt%) [16].

PMMA/MWCNT/Ag hybrid composites plotted against each other at different ratios showed the exponential factor (s). As seen in **Table 1**, the values of s for all composite samples are quite small. As a result, it can be concluded that conductivity occurs during hopping. However, the exponents fluctuate as the filler content varies, and increases in exponents are attributed to the increase in charge carriers caused by the addition of MWCNT and Ag. The results showed that between 10 kHz and 10 MHz, the "total" climbs as frequency increases.

All of the PMMA/MWCNT/Ag hybrid composites have had their dielectric characteristics examined. For all of the composites, **Figs. 4a** and **4b** depict the frequency-dependent fluctuation in dielectric constant and dielectric loss. Ag at an increase in frequency with a drop of and" at high concentrations, and the higher frequency loss becomes virtually constant at lower MWCNT concentrations. Because there are two types of dielectric losses, this suggests that dipoles organize themselves along field direction at low frequencies to increase overall polarization. The first is known as conduction loss and is caused by the actual charge flowing into the dielectric. The second is known as dielectric loss and is caused by molecules' or atoms' spins in an alternating current field [21, 22].

Figure 4c illustrates how the value of the loss tangent rises with frequency, reaches a maximum at a certain frequency, and then falls at higher frequencies. The lack of dielectric materials to follow the applied electric field causes a loss tangent to arise, which is characterized by the generation of heat.

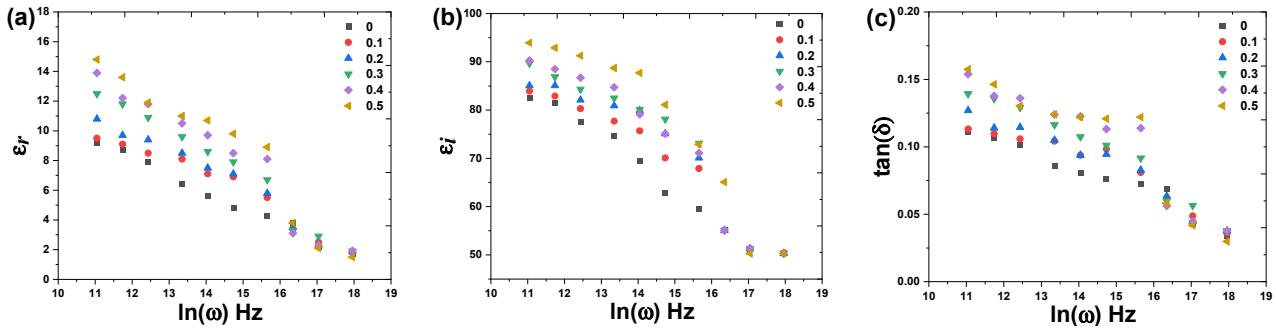

Figure 4. (a) real (ε_r), **(b)** imaginary (ε_i) parts of dielectric constant, and **(c)** loss tangent (tan(δ) versus ln(ω) at the temperature of 323 K for pure PMMA and PMMA/MWCNT/Ag hybrid composites with ratios of MWCNTs of 0.1, 0.2, 0.3, 0.4, and 0.5 wt%.

Electromagnetic Interference shielding (EMI)

High reflection and low absorption should generally define the EMI shielding material. The best course of action in this situation is to apply a few layers of the copper-filled composite material that reflects light, as illustrated in **Fig. 5** The SE of EMI of PMMA/MWCNT/Ag hybrid composites increased with MWCNT and Ag content because carbon nanotubes (CNTs) comprise electrically conducting organic nanomaterials, and their composite displays significant

EMI shielding capabilities. By layering 0.1 mm thick MWCNT/Ag/PMMA composite films, it was feasible to achieve EMI shielding effectiveness of up to 19 dB in the frequency range of 8.2-12.4 GHz (X-band).

The different carbonaceous fillers' EMI shielding capabilities are in-depth studied. In the live broadcasting, entertainment, aviation, and defense industries, electromagnetic interference (EMI) has been a major source of worry since it can worsen while critical radio signals are present. Due to their flexibility, low density, high mechanical strength, high thermo-stability, high electrical and thermal conductivity, outstanding fracture toughness, and high friction/wear resistance, organic polymeric composites containing carbonaceous fillers are frequently employed to lessen the impact of EMI. Many carbon-based materials, both in mono and compound form, are employed as EMI shielding materials. Although increasing the number of MWCNT would increase the shielding capacity, doing so would make it more difficult to produce composites with large MWCNT volume fractions. By including 0.5 wt% of Ag in all composites, these flaws may be fixed, and the superior conductivity of silver is retained while still enhancing the interfacial contact of MWCNT, which agrees with other works [16,17].

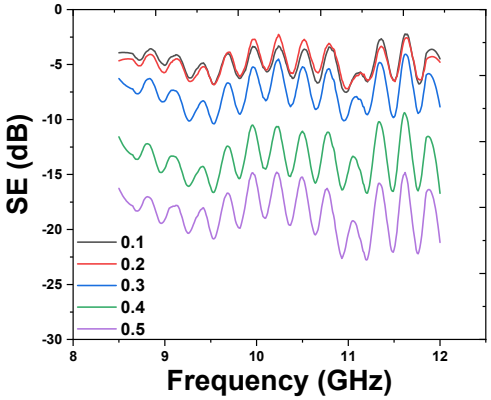

Figure 5. Electromagnetic interference (EMI) shielding (SE) versus frequency for PMMA/MWCNT/Ag hybrid composites with ratios of MWCNTs of 0.1, 0.2, 0.3, 0.4, and 0.5 wt%.

Hybrid particles, which were created by fusing metal and polymer, have shown advantageous qualities including conductive composite, EMI shielding, electromagnetic wave absorption, catalysts, batteries, and sensors. The metal with specified electrical conductivity properties can be used in a variety of industrial applications, including shielding against radio frequency interference (RFI), electrostatic discharge (ESD), electrically conductive adhesives, and circuit components in microelectronics. Silver is the single metal with the highest electrical conductivity, and unlike other metals, its oxide form is also electrically conductive. These benefits have led to silver's predominant use in a variety of sectors as a polymer/silver composite. However, the volume proportion of silver was spread in the polymer matrix to achieve excellent electrical conductivity.

One of the practical approaches favored for material characterization is TGA-DTA. Using this method, changes brought about by breakdown, transformation, and formation processes during a controlled heating process may be examined. Samples were heated at a rate of 5C/min from ambient temperature to 350°C. The endothermic action shows the elimination of the chemically bonded water at higher temperatures of 200–300°C. The exothermic effect discovered in the temperature range of 200 to 350°C was attributed to the combustion of organic materials that weren't completely burned during firing in reducing conditions and transformed into carbonaceous particles, which are believed to have been purposefully added into the PMMA. The thermal degradation of PMMA in an oxygen-containing environment (O_2, Air) initially results in an increase in the PMMA thermal stability as the temperature for the commencement of mass loss rises by 50°C and 70°C. A gas-containing atmosphere (Air) destabilizes the PMMA at about 230–250°C, accelerating the thermal breakdown process.

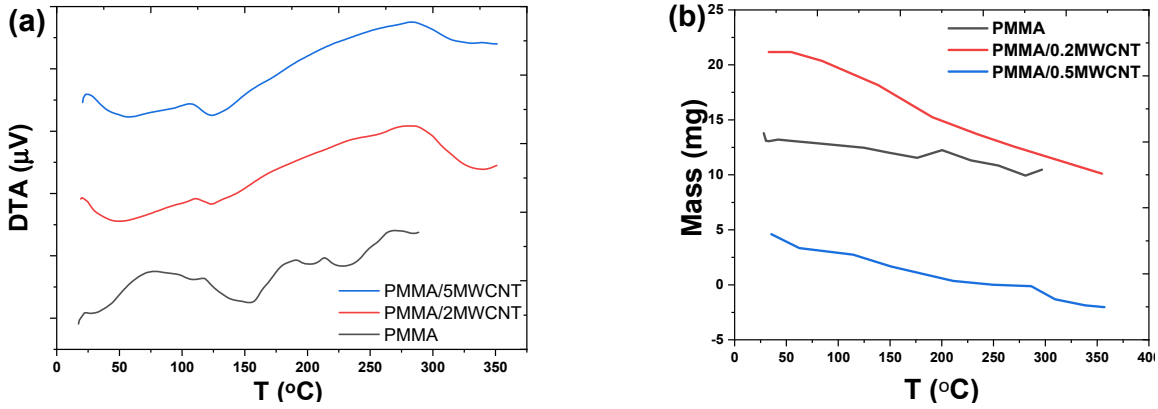

Figure 6. (a) Differential Thermal Analysis (DTA) and **(b)** mass versus temperature (T) for pure PMMA and PMMA/MWCNT/Ag hybrid composites

The melting peak changes to lower temperatures emerge at (153.84°C, 121.45°C, and 125.67°C) in **Figs. 6a** and 6**b** DTA and TGA curves of pure PMMA and PMMA/MWCNT/Ag. These curves exhibit one mass endothermic peak that represented the melting point of the raw materials (PMMA, MWCNT, and Ag). The curve also demonstrates a significant endothermic reaction beginning at 114°C and continuing to 140°C. The level of adsorption is typically higher than the molar mass of the PMMA. This is predicted because just a portion of the polymer chain was adsorbed,

whereas the remaining chain is more likely to bind to the MWCNT surface by CH interactions. The MWCNTs exhibit minimal mass loss owing to the presence of amorphous carbon and other impurities and are thermally stable across the whole temperature range investigated (up to 600°C) [20]. Additionally, when the accessible MWCNT surface area increases, more polymer may adsorb, which leads to PMMA adsorption when the number of MWCNTs is increased. The PMMA/MWCNT/Ag sample's TGA/DTA diagrams show a weight loss as a result of the carbon layer's thermal degradation, which begins at 279–309°C and 278–305°C, respectively. The DTA diagram's exothermic peak, which is located at 288°C and 290°C, respectively, denotes the exothermic curves caused by the crystalline phase of composites and thermal breakdown. The DTA plot shows a large endothermic peak between 200 and 300°C, which is mostly due to the crystallization of additional silver nanoparticles to hybrid PMMA/MWCNT. The DTA profiles show that the material completely cooled and crystallized at the same time.

The properties associated with polymer matrix composites are the functions of the filler size, shape, dispersion and the matrix and filler interactions. In this work the filler shape and size is same throughout the experiments. The main purpose of FESEM is to check the degree of dispersion and filler matrix interaction. The FESEM analysis surface morphology of the samples shows the micrographs of pure PMMA and PMMA/MWCNT/Ag at 0.1/0.5 concentration is showing good dispersion into the matrix dispersed in PMMA. From the Figures it is observed that dispersed MWCNT, Ag filler particle creates considerable change in the morphology of the pure PMMA film. The SEM images of the pure PMMA shows a pores and granular structure while the MWCNT, Ag dispersed PMMA matrix exhibits a smoother and more compact amorphous surface morphology, i.e., no major cracks were obtained. It is important to mention that the PMMA particles retained their exhibit spherical morphology after being deposited and cured because they weren't fully melted during the heating process for the film formation. the good dispersion of Ag-NPs results in an essential enhancement in the properties of the fabricated PMMA/Ag nanocomposites. The FESEM image of the hybrid composite fi lm shows a homogeneous dispersion of MWCNTs, Ag in PMMA (Fig. 7) with no aggregation of nanotubes even with 0.5/0.5% loading which suggests that ultra-sonication is quite useful in dispersion of the tubes in PMMA that enhanced electrical properties and showed high electrical conductivity and EMI shielding properties.

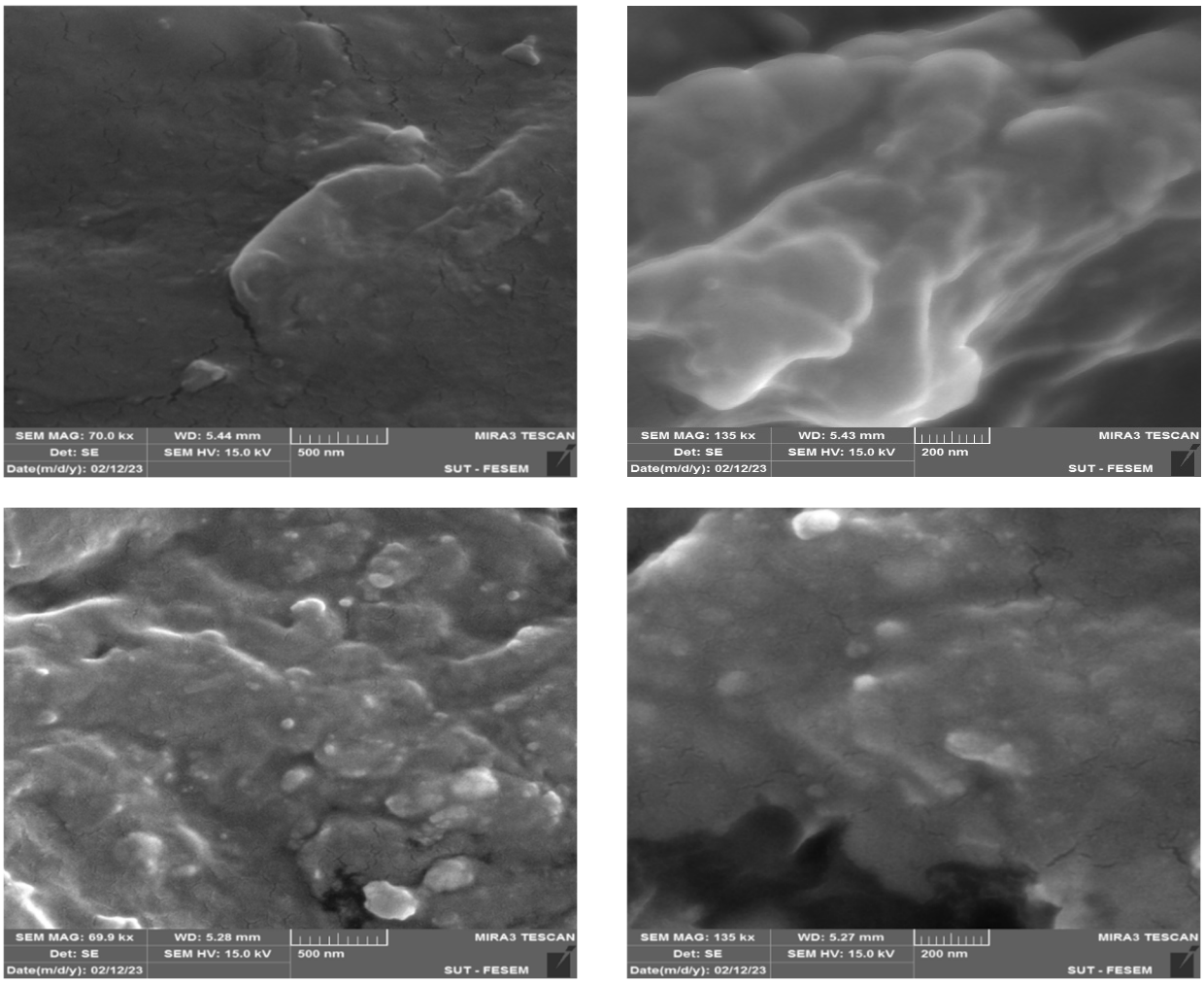

Figure 7. Field Emission Scanning Electron Microscope (FESEM) for pure PMMA and PMMA/MWCNT/Ag hybrid composites

Figure 7 showed that the fabricated Ag-materials were of a mean size of about 30 nm i.e. Ag-NPs were dispersed in PMMA/MWCNT/Ag nanocomposites and led to well significant results on the various characteristics of PMMA//MWCNT/Ag nanocomposites such as electrical, thermal, shielding properties. Homogeneous dispersion of Ag-NPs is preferred to avoid the formation of crack creativities in the PMMA/MWCNT nanocomposites loaded (0.5%wt) on the distribution and the dispersion of the Ag-NPs as nanofiller in the PMMA/MWNT/Ag nanocomposites matrix.

3. CONCLUSION

PMMA/MWCNT/Ag hybrid composite display electrical conductivity of around 2.14×10^{-4} S/cm as a percolation critical concentration is obtained at 0.5 wt% for MWCNT and 0.5 wt% for Ag. Dielectric properties have been tested across a wide frequency range. The AC conductivity varies with variations in MWCNT and Ag concentrations, as well as with applied field frequency and dielectric constant, illustrative of the significantly improved permittivity of these hybrid composites. Increased frequency causes a reduction in the dielectric constant, dielectric loss, loss of tangent, and dielectric loss. The PMMA/MWCNT/Ag hybrid composite's shielding performance is significantly influenced by the weight proportion (0.5 wt%/0.5 wt%) of MWCNT and Ag, which increases the X-band shielding efficiency. According to TGA/DTA research, exothermic reactions cause the majority of weight loss between 200 and 300°C. FESEM show that PMMA/MWCNT/Ag hybrid composites had uniform dispersion of the carbon nano tube and silver particles within the PMMA matrix that due to filler presents large surface area for better interfacial bonding between the matrix and particles.

• **Funding**
No funding that personal for the student MSc.
• **Author Contribution**
Nadia Abbas Ali wrote the main manuscript text and Badiaa Alaw prepared figures and Tables and collected the data
• **Conflict of Interest**
- All authors have participated in (a) conception and design, or analysis and interpretation of the data; (b) drafting the article or revising it critically for important intellectual content; and (c) approval of the final version.
- This manuscript has not been submitted to, nor is under review at, another journal or other publishing venue.
- The authors have no affiliation with any organization with a direct or indirect financial interest in the subject matter discussed in the manuscript

• **Data Availability Statement**
- Deposit your research data in a relevant data repository

ORCID IDs

Nadia Abbas Ali, https://orcid.org/0000-0002-3996-112X

REFERENCES

[1] R.S. Yadav, I. Kuritka, and J. Vilcakova, *Advanced Spinel Ferrite Nanocomposites for Electromagnetic Interference Shielding Applications*, (Elsevier, 2020).
[2] A. Sami, and M.E. Abdulmunem, "Synthetic Aperture Radar Image Classification: a Survey," Iraqi Journal of Science, **61**(5), 1223-1232 (2020). https://doi.org/10.24996/ijs.2020.61.5.29
[3] A.A. Kareem, and H.Kh. Rasheed, "Electrical and thermal characteristics of MWCNTs modified carbon fiber/epoxy composite films,," Materials Science Poland, **37**(4), (2019). https://doi.org/10.2478/msp-2019-0081
[4] H. Lecocq, N. Garois, O. Lhost, P.-F. Girard, P. Cassagnau, and A. Serghei, "Polypropylene/carbon nanotubes composite materials with enhanced electromagnetic interference shielding performance: Properties and modeling," Composites Part B: Engineering, **189**, 107866 (2020). https://doi.org/10.1016/j.compositesb.2020.107866
[5] H. Wang, K. Zheng, X. Zhang, X. Ding, Z. Zhang, C. Bao, L. Guo, et al., "3D network porous polymeric composites with outstanding electromagnetic interference shielding," Composites Science and Technology, **125**, 22-29 (2016). http://dx.doi.org/10.1016%2Fj.compscitech.2016.01.007
[6] A.N. Abd, A.H. Al-Agha, and M.A. Alheety, "Addition of Some Primary and Secondary Amines to Graphene Oxide, and Studying Their Effect on Increasing its Electrical Properties," Baghdad Science Journal, **13**(1), (2016). https://doi.org/10.21123/bsj.2016.13.1.0097
[7] A.M. Abd-Elnaiem, S.I. Hussein, H.S. Assaedi, and A.M. Mebed, "Fabrication and evaluation of structural, thermal, mechanical and optical behavior of epoxy–TEOS/MWCNTs composites for solar cell covering," Polym. Bull. **78**(7), 3995-4017 (2021). https://doi.org/10.1007/s00289-020-03301-5
[8] D. Yuan, H. Guo, K. Ke, and I. Manas-Zloczower, "Recyclable conductive epoxy composites with segregated filler network structure for EMI shielding and strain sensing," Composites Part A: Applied Science and Manufacturing, **132**, 105837 (2020). https://doi.org/10.1016/j.compositesa.2020.105837
[9] Z. Zeng,W. Li, N. Wu, S. Zhao, and Xuehong Lu, "Polymer-assisted fabrication of silver nanowire cellular monoliths: toward hydrophobic and ultraflexible high-performance electromagnetic interference shielding materials," ACS applied materials & interfaces, **12**(34), 38584-38592 (2020). https://doi.org/10.1021/acsami.0c10492
[10] S. Ghosh, S. Ganguly, P. Das, T.K. Das, M. Bose, N.K. Singha, A.K. Das, and N.C. Das, "Fabrication of reduced graphene oxide/silver nanoparticles decorated conductive cotton fabric for high performing electromagnetic interference shielding and antibacterial application," Fibers and Polymers, **20**, 1161-1171 (2019). https://doi.org/10.1007/s12221-019-1001-7
[11] F. Ren, Z. Li, L. Xu, Z. Sun, P. Ren, D. Yan, and Z. Li, "Large-scale preparation of segregated PLA/carbon nanotube composite with high efficient electromagnetic interference shielding and favourable mechanical properties," Composites Part B: Engineering, **155**, 405-413 (2018). https://doi.org/10.1016/j.compositesb.2018.09.030

[12] H. Gargama, A.K. Thakur, and S.K. Chaturvedi, "Polyvinylidene fluoride/nanocrystalline iron composite materials for EMI shielding and absorption applications," Journal of Alloys and Compounds, **654**, 209-215 (2016). https://doi.org/10.1016/j.jallcom.2015.09.059
[13] H.M. Kim, K. Kim, C.Y. Lee, J. Joo, S.J. Cho, H.S. Yoon, D.A. Pejaković, et al., "Electrical conductivity and electromagnetic interference shielding of multiwalled carbon nanotube composites containing Fe catalyst," Applied physics letters, **84**(4), 589-591 (2004). https://doi.org/10.1063/1.1641167
[14] S.-M. Yuen, C.-C.M. Ma, C.-Y. Chuang, K.-C. Yu, S.-Y. Wu, C.-C. Yang, and M.-H. Wie, "Effect of processing method on the shielding effectiveness of electromagnetic interference of MWCNT/PMMA composites," Composites Science and Technology, **68**(3-4), 963-968 (2008). https://doi.org/10.1016/j.compscitech.2007.08.004
[15] Y. Liu, D. Song, C. Wu, and J. Leng, "EMI shielding performance of nanocomposites with MWCNTs, nanosized Fe3O4 and Fe," Composites Part B: Engineering, **63**, 34-40 (2014). http://dx.doi.org/10.1016/j.compositesb.2014.03.014
[16] H. Yuan, Y. Xiong, Q. Shen, G. Luo, D. Zhou, and L. Liu, "Synthesis and electromagnetic absorbing performances of CNTs/PMMA laminated nanocomposite foams in X-band," Composites Part A: Applied Science and Manufacturing, **107**, 334-341 (2018). https://doi.org/10.1016/j.compositesa.2018.01.024
[17] N.C. Das, Y. Liu, K. Yang, W. Peng, S. Maiti, and H. Wang, "Single-walled carbon nanotube/poly (methyl methacrylate) composites for electromagnetic interference shielding," Polymer Engineering & Science **49**(8), 1627-1634 (2009). https://doi.org/10.1002/pen.21384
[18] H.K. Al-Lamy, E.M. Nasir, H.J. Abdul-Ameer, "Electrical properties of Cdxse1-x films at different thickness and annealing temperatures," Digest Journal of Nanomaterials and Biostructures, **15**(1), 143-156 (2020). https://chalcogen.ro/143_LamyHK.pdf
[19] A.H. Mohammed, A.N. Naje, and R.K. Ibrahim, "Photoconductive Detector Based on Graphene Doping with Silver Nanoparticles," Iraqi Journal of Science, **63**(12), 5218-5231 (2022). https://doi.org/10.24996/ijs.2022.63.12.12
[20] ASTM D4935-10, *Standard Test Method for Measuring the Electromagnetic Shielding Effectiveness of Planar Materials*, (2010).
[21] A.F. Ahmad, S.A. Aziz, S.J. Obaiys, M.H.M. Zaid, K.A. Matori, K. Samikannu, and U.S. Aliyu, "Biodegradable poly (lactic acid)/poly (ethylene glycol) reinforced multi-walled carbon nanotube nanocomposite fabrication, characterization, properties, and applications," Polymers, **12**(2), 427 (2020). https://doi.org/10.3390/polym12020427
[22] A.S. Abd-Alsada, and M.F.A. Alias, "Impact of CNT Concentrations on Structural, Morphological and Optical Properties of ZnO: CNT Nano composite Films," Journal of Physics: Conference Series, **2114**(1), 012020 (2021). https://doi.org/10.1088/1742-6596/2114/1/012020
[23] I.M. Ali, A.A. Mohammed, and A.H. Ajil, "A study of the characterization of CdS/PMMA nanocomposite thin film," Iraqi Journal of Physics, **14**(29), 191-197 (2016). https://www.iasj.net/iasj/pdf/c3192b6d984e4477

ПІДВИЩЕННЯ ЕКРАНУЮЧОЇ ЕФЕКТИВНОСТІ ГІБРИДНОГО КОМПОЗИТУ PMMA/MWCNTS/Ag ДЛЯ ЗАСТОСУВАННЯ В X-ДІАПАЗОНІ

Бадіа Ісмал Алаві, Надя Аббас Алі
Факультет фізики, Науковий коледж, Багдадський університет, Багдад, Ірак

Гібридні композитні плівки багатошарові поліметилметакрилат/вуглецеві нанотрубки зі сріблом (PMMA/MWCNT/Ag) одержані методом лиття з розчинника для використання в електротехніці. Провідність змінного струму і діелектричні характеристики були досліджені при кімнатній температурі. Електропровідність гібридного композиту досягає критичної концентрації перколяції $2{,}14\times10^{-4}$ см/см за рахунок легування Ag. Для всіх гібридних композитів PMMA/MWCNT/Ag частотно-залежна діелектрична проникність зменшується з розширенням діапазону частот. Зі збільшенням концентрації MWCNT та Ag провідність змінного струму має тенденцію до збільшення. Встановлено, що зміст MWCNT та Ag істотно впливає на SE даних композитів. Високу ефективність електромагнітного (ЕМ) екранування (SE) було досягнуто в діапазоні частот від 8,2 до 12,4 ГГц (X-діапазон). Максимальне ЕМ згасання у 18 дБ на частоті 12 ГГц було досягнуто при використанні 0,5 мас.% MWCNT та Ag. Термічний аналіз сформованих гібридних композитів PMMA/MWCNT/Ag показав, що екзотермічні реакції з найбільшою втратою маси протікають в інтервалі температур від 200°C до 300°C. Скануючий електронний мікроскоп з польовою емісією (FESEM) показує, що гібридні композити PMMA/MWCNT/Ag мають однорідну дисперсію вуглецевих нанотрубок та частинок срібла у матриці PMMA.

Ключові слова: *екранування електромагнітних перешкод; X-діапазон; електрична провідність; діелектрична постійна; діелектричні втрати; термічний аналіз*